EUROFUSION WPJET1-CP(16) 15035

B Ding et al.

Recent experimental and modeling advances in the understanding of lower hybrid current drive in ITER-relevant regimes

Preprint of Paper to be submitted for publication in
Proceedings of 26th IAEA Fusion Energy Conference

This work has been carried out within the framework of the EUROfusion Consortium and has received funding from the Euratom research and training programme 2014-2018 under grant agreement No 633053. The views and opinions expressed herein do not necessarily reflect those of the European Commission.

Recent experimental and modeling advances in the understanding of lower hybrid current drive in ITER-relevant regimes

B J Ding1), P Bonoli2), A Tuccillo3), M Goniche4), K Kirov5), M Li1), Y Li1), R Cesario3), G Wallace2), Y Peysson4), A Ekedahl4), L Amicucci3), R Parker2), S Shiraiwa2), I Faust2), S Baek2), A Cardinali3), C Castaldo3), S Ceccuzzi3) J Mailloux5), F Liu1), B Wan1), JET Contributors*

1) Institute of Plasma Physics, Chinese Academy of Science, Hefei 230031, P R China
2) MIT Plasma Science and Fusion Center, Cambridge, Massachusetts 02139, USA
3) ENEA, FSN Department, C. R. Frascati, via E. Fermi 45, 00044 Frascati (Roma), Italy
4) CEA, IRFM, F-13108, St-Paul-Lez-Durance, France
5) CCFE, Culham Science Centre, Abingdon, Oxon, OX14 3DB, UK
EUROfusion Consortium, JET, Culham Science Centre, Abingdon, OX14 3DB, UK
Email: bjding@ipp.ac.cn

Abstract Progress in understanding lower hybrid current drive (LHCD) at high density has been made through multi-machine experiments and modeling, focused on application in ITER. The dimensionless parameter that characterizes LH wave accessibility and wave refraction shows these experiments bracket the region in parameter space where ITER LHCD experiments would operate in the steady state scenario phase. The driven current in the core has been enhanced by reducing neutral density at the plasma edge. The edge temperature is thereby increased and the effects of parametric instability (PI) and collisional absorption (CA) are reduced. The effect of PI is also mitigated by higher LH operating frequency. These effects, plus stronger single-pass damping that will lessen the effects of CA, all points favorably to the application of LHCD in ITER.

1. Introduction

Lower hybrid current drive (LHCD) has the attractive property of high off-axis ($r/a \approx 0.7$) current drive efficiency making this a useful technique for broadening the current density profile in order to create non-monotonic (shear reversed) profiles of the safety factor – q(r) with $q_{min} > 2$ and large shear reversal radius ($r/a \approx 0.7$). The resulting profiles of safety factor allow access to improved energy confinement regimes with high fractions of the non-inductive bootstrap current (≈ 60-70%) [1], thus enabling achievement of the steady state Scenario-4 in the ITER device. However, how to improve LHCD capability at high density is an important issue to be solved before this application. Experiments on FTU identified a new method that enabled for the first time producing LHCD at densities even higher than in ITER [2]. This method was assessed on the basis of previous theoretical predictions of diminished parasitic effect of spectral broadening due to parametric instability (PI) under higher temperature of plasma edge [3]. In further studies, collisional absorption (CA) [4], and scattering from density fluctuations (SDF) [5, 6], individually or in combination, were also proposed as possible candidates for the current drive (CD) efficiency decreasing at high density faster than standard theory prediction [7]. A multi-machine assessment, including experiments and modeling in EAST, Alcator C-Mod, JET tokamaks, has been continued as a joint activity under the coordination of the Integrated Operation Scenarios (IOS) Topical

* See the author list of "Overview of the JET results in support to ITER" by X. Litaudon et al. to be published in Nuclear Fusion Special issue: overview and summary reports from the 26th Fusion Energy Conference (Kyoto, Japan, 17-22 October 2016)

2. Joint experimental activity

21. EAST EAST experiments aim at fully assessing conditions useful for enabling the LHCD effect into dense plasma core. As shown in Fig.1, first LHCD results [8] with 4.6GHz show that the lower hybrid wave (LHW) can be coupled to plasma with low reflection coefficient, drive plasma current, modify plasma current profile, and heat plasma efficiently. Meanwhile, good plasma heating is observed with core electron temperature above 4keV [8]. The effect of lower hybrid (LH) frequency, with $N_{//}^{peak}$=2.1 for 2.45GHz and $N_{//}^{peak}$=2.04 for 4.6GHz) and comparable directivities of the spectrum (0.74***vs***0.76), on LHCD characteristics (n_e =2.0×$10^{19}$$m^{-3}$) with a same coupled power (1.05MW) in a lower single null (LSN) configuration was investigated in EAST (see Fig. 2) [9]. It shows the residual voltages (V_{loop}) are 0.27V and 0.15V, respectively, during 2.45GHz and 4.6GHz application, implying a better CD efficiency for 4.6GHz LH waves. Better plasma heating effect for 4.6GHz can be seen from the time evolution of plasma stored energy, and central electron temperature (T_{e0}) measured with a X-ray Crystal Spectrometer (XCS) [10]. The internal inductance (li) is higher with the 4.6GHz LH wave injection, meaning a more peaked current profile. The plasma rotation shows, for similar power input, a larger central rotation change with 4.6GHz. The temperature at divertor induced from the infrared radiation (IR) shows higher temperature with 4.6GHz wave, possibly due to larger plasma radiation.

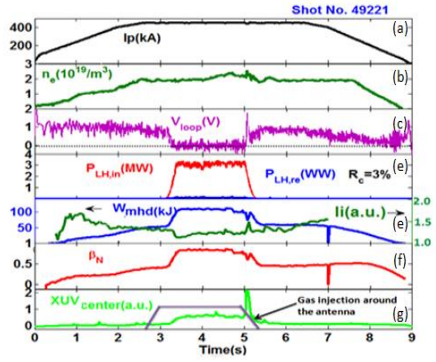

Fig. 1 Typical waveform of coupling, current drive and plasma heating(4.6GHz)

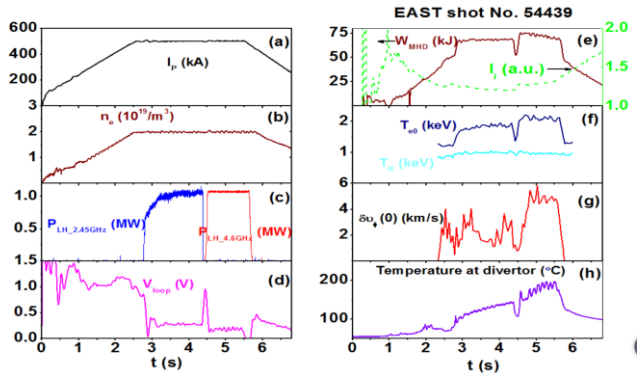

Fig. 2 Typical waveform of LH frequency effect on plasma characteristics

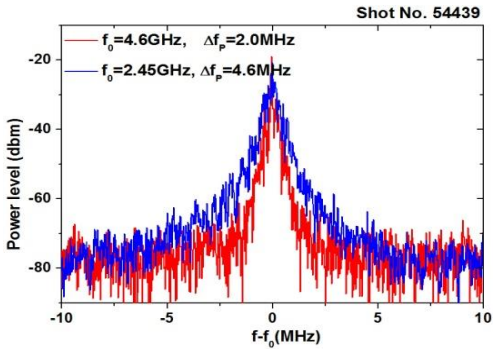

Fig. 3 PI signal by RF

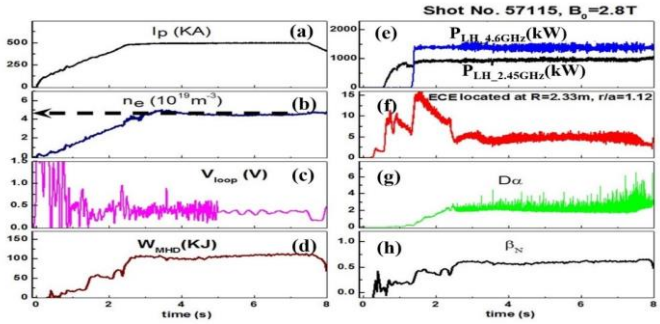

Fig. 4 H-mode with LHCD at high density

Above experimental results show that LHWs at 4.6 GHz exhibit stronger CD capability than at 2.45 GHz, in agreement with less pronounced PI behavior with 4.6GHz LH wave (see Fig. 3). By means of 4.6GHz and 2.45GHz LHCD systems, as shown in Fig. 4, H-mode is

obtained at relatively high density, even up to n_e~4.5 × $10^{19}m^{-3}$, and a current drive effect is still observed.

2.2 Alcator C-Mod On Alcator C-Mod, the LH RF physics program focuses on improving the CD at high density and understanding how to properly extrapolate present experiments to a reactor. The power deposition of LH waves into the edge plasma of a diverted tokamak has been systematically measured for the first time in the experiment. By means of fast time resolution edge diagnostic sets including innovative fast-thermocouples, an extensive set of Langmuir probes, and a Ly-alpha ionization camera, LH power modulation reveals that ~75% of the LH power is deposited very close to or outside of the last closed flux surface (LCFS) at n_e~1.1 × $10^{20}m^{-3}$. The loss of CD at high density correlates with the existence of a cold, dense and collisional divertor plasma [11].

In a reactor, LH waves will experience strong single pass absorption, and therefore, the direct interaction with cold dense divertor plasmas due to multiple passes discussed above can be minimized naturally. However, LH waves still must propagate a significant length in the poloidal/toroidal directions through the SOL plasmas before crossing the LCFS. A suite of new diagnostics is installed to better characterize the LH wave propagation during this first pass from the launcher to core. Two sets of RF magnetic probe arrays are installed at different toroidal locations which are magnetically mapped to the launcher. In addition, a new Stark Effect Lower Hybrid Field (SELHF) spectrometer [12] is also installed to measure the LH wave field in front of the LH launcher in collaboration with Oak Ridge National Laboratory.

Figure 5 shows the LH wave power as a function of density measured by one of new RF probe arrays [13]. A reduction of LH power at the launched frequency (4.6 GHz) is observed in all three discharges with different plasma currents. The highest current case shows smaller reduction of LH power compared to other two. This trend is consistent with the recovery of current drive at high current [14], suggesting that significant modification of the wave spectrum occurs during the first pass and may be responsible for the loss of current drive. Figure 5 also shows the signal strength at 4.57 GHz, showing the spectrum power in this frequency range increases to about 10 dB below the peak power as the density increases. Note that the 4.57 GHz data shown in the figure corresponds to the ion-cyclotron PI sideband LH waves. In contrast to ion-sound PI's, which are stabilized with collisional absorption [15], those decay waves corresponding to the ion-cyclotron side bands remain unstable for a wide range of edge parameters found in various tokamaks and can be responsible for increased parasitic power losses universally observed in various LH experiments.

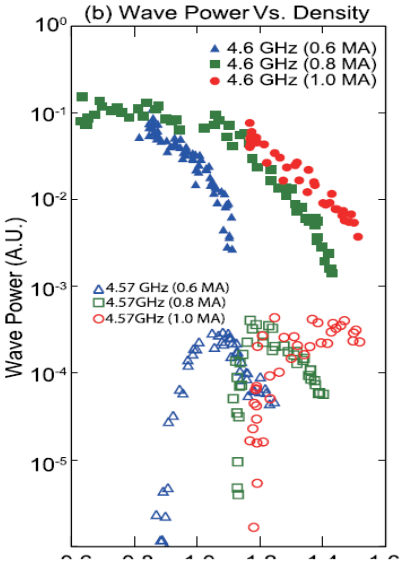

Fig.5 *Wave power measured with the three probe array as a function of the line-averaged density at three different plasma currents. [Ref. 13].*

2.3 JET On JET, as shown in Fig.6, for plasmas in weakly accessible conditions, the magnitude of fast electron tail drops, as it does on C-Mod or Tore Supra when the density is normalized to $n_{\text{e-accessibility}}$. However the role of LH wave accessibility is difficult to assess in

Fig. 6. For example, the HXR data of EAST ('poor lithium' case) with 2.45GHz system indicates a similar decay of the fast electron tail for ne >2x10^{19}m^{-3} although the LH waves could penetrate deeper in the plasma [16]. Thus LH wave accessibility would not necessarily play a significant role in those discharges as indicated by similar behavior of fast electron data in inaccessible/accessible conditions [17]. Recent time dependent ray tracing / Fokker Planck analysis [18] has indicated that loss of wave accessibility at high density in JET could be partially responsible for a reduction in the LHCD effect; however this analysis relies on multiple passes of the LH wavefront between the slow wave cut-off and the confluence layer between the slow and fast wave modes in plasma. However, detailed analysis of spectral broadening via the PI effect has shown that this mechanism is a strong candidate for the decrease in HXR emission since the density at large radii in these discharges exceeds a critical value of ≈ 4 x10^{19}m^{-3}, which promotes conditions of cold plasma edge that favours the undesired effect of PI spectral broadening [2, 17].

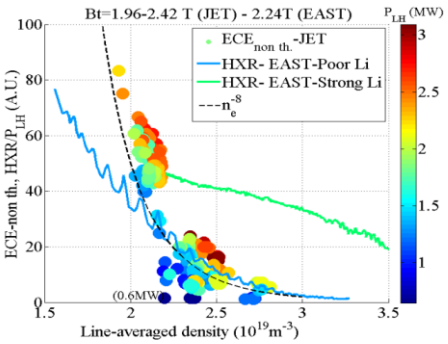

Fig. 6 ECE$_{nonth.}$(JET) and HXR (EAST) as a function of n_e

3. Cross-study and data analysis

Modeling of PI, CA and SDF in EAST have shown that these mechanisms could be responsible for the larger decrease of CD efficiency than theory predication at high density [19]. Modeling of PI using the LHPI code [20] and the MIT code [21, 22] are qualitatively consistent with the measured RF spectrum. In MIT, a growth-rate solver originally based on the parametric dispersion relation derived by Porkolab [23] has been extended [22] to include another form of the dispersion following the approach in Liu [24]. Using this solver, recent investigations have focused on the parametric excitation of the LH wave (sideband) in the parallel coupling limit. In this limit, the excited sideband LH wave can propagate nearly along the launched LH pump wave. Since the sideband can be excited and its amplitude can grow only in the presence of the pump, this parallel coupling case could result in a higher sideband amplitude in the high density plasma in which the pump wave has a limited radial penetration and spends longer time at the plasma edge where unstable to parametric instabilities. Figure 7 shows an example of the normalized sideband frequency (ω_R/ω_{ci}) and growth rate (γ/ω_{ci}) spectra when $\theta = 10$ deg in EAST. In this particular case, one interesting feature is the appearance of a dip in the growth rate spectrum around the ion cyclotron first-harmonic solution ($k\lambda_{De} \approx 0.06883$). This dip is due to the upper sideband also being nearly resonant ($|\epsilon^+| \approx 0$), which is generally off-resonant and does not contribute much in determining γ in the limit $\theta \to 90$ deg.

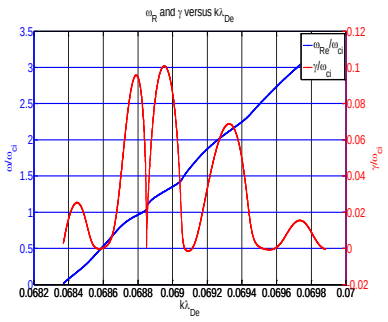

Fig. 7 Growth rate (f_0 = 2.45 GHz, n_e=3x10^{18} m^{-3}, T_e=T_i=50 eV, B=2.8T, $ck_{||0}/\omega_0$=2.1, $ck_{||}/\omega_0$=7, P = 3.2 MW/m^2)

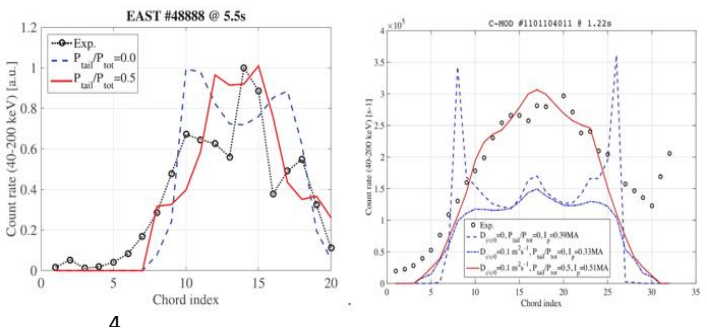

Fig. 8 Comparison between Exp. and Calc. (C3PO/LUKE) with and w/o spectrum broadening (left: EAST, right: Alcator C-Mod)[Ref. 27]

Measurements indicate there is little change in the LH power density profile in the density range where good current drive is obtained. Furthermore the simulated profiles of driven current density, power deposition, and hard x-ray emission do not always agree with experimental measurements in Alcator C-Mod [25] and Tore Supra [26], with the simulated profiles being off-axis and hollow compared to those in the experiment. The existence of a "tail" in the launched power spectrum due to SDF, considered in C3PO/LUKE, greatly reduces model sensitivity to plasma conditions while at the same time significantly improves the consistency between modeling and experiments in plasma conditions for which the spectral gap is large in EAST and Alcator C- Mod [27], as well as in the Tore Supra tokamak (see Fig. 8). The spectral modifications employed in C3PO / LUKE typically place ≤ 50% of the incident LH power in a "tail" that extends from $2 \leq n_{//} \leq 5$ and that is modeled by a series of smaller gaussian power lobes, whereas the "tail" model employed in GENRAY / CQL3D places 5-10% of the incident LH power in smaller gaussian power lobes at $n_{//} \approx$ 2.5-2.7. An example using GENRAY/CQL3D for the EAST tokamak is shown in Fig. 9, showing that a relocation of 10% of total LH power to modestly high $N_{||}$ (~2.7) gives the best fit to the experimental HXR emission profile shape. At this time the differences needed in the spectral broadening in C3PO/LUKE and GENRAY/CQL3D in order to improve agreement with experiment are under study. Simulations of CA using GENRAY/CQL3D suggest that SOL plasmas can have significant impact on current drive when single pass absorption is weak [29]. Recently a model which takes into account realistic SOL geometry and the existence of a cold dense plasma near the divertor was implemented in GENRAY. This improved model for the SOL predicts a more significant reduction of current drive as the density is increased compared to previous work [28] and is more consistent with experiment [29] (see Fig. 10).

Fig. 9 Comparison of HXR emission profile and current profile prediction (GENRAY/CQL3D), experiment (blue), simulation with(green) and w/o (red) spectral spreading (EAST #48888 at 5.5s.)

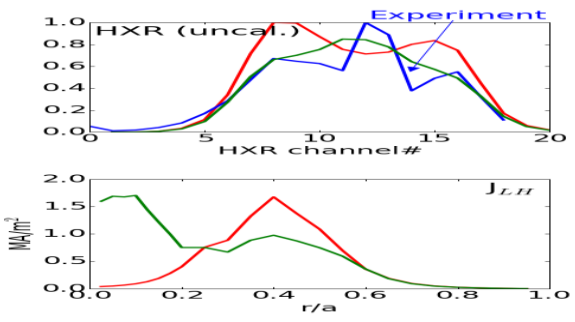

Fig. 10 GENRAY/CQL3D prediction of HXR emission intensity when 2D realistic SOL is used (blue).

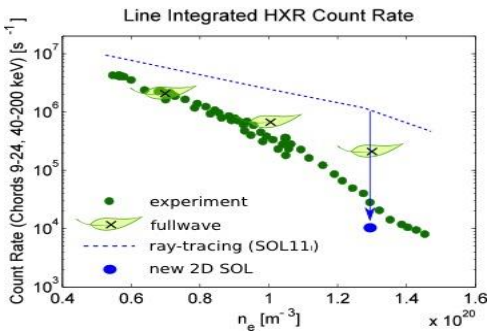

Previous experiments on FTU indicated that SDF would not play a significant role in tokamak experiments performed so far at high plasma densities, since LHCD effects occurred at very high density (n_e=2 × $10^{20}$$m^{-3}$). With an ITER-relevant n_e profile and high T_e periphery regime, the RF probe spectrum was symmetrically broadened (up to 7 MHz), attributable to SDF [2]. Conversely, a significantly broadened and downshifted spectrum (up to 15 MHz), not accompanied by any LHCD effect in plasma was produced in standard high-density regime, consistent with PI modelling results [2]. Therefore, the cause of the reduction of the LHCD at high density has not been conclusively shown from the FT-U experiments alone.

Based on the experiments in Sec. 2.1, the effect of LH frequency (2.45 GHz and 4.60 GHz) on PI in EAST has been analysed. Considering the typical EAST plasma with a line-averaged plasma density of 2x10^{19} m^{-3} and using the LHPI code, the calculated frequencies and growth rates of PI driven mode are shown in Fig.11, in which the RF coupled power of 1MW, the antenna power spectrum peak ($n_{//0}$ =2.0) and the EAST antenna dimensions have been considered. For the pump frequency of 4.60 GHz, the analysis performed by the LHPI code shows that the PI mechanism is mostly driven by a low frequency quasi-mode having a maximum homogeneous growth rate ($\gamma / \omega_0 \approx 4x10^{-4}$) that is slightly smaller (of about 20%) than that for 2.45 GHz. The calculation is qualitatively consistent with PI modelling (see Fig. 12) with the MIT code, showing that growth rate is positive and finite with a peaking near the first ion cyclotron harmonic for both case but reduces by a half at 4.6 GHz. Calculation suggests PI could be different for the two frequencies.

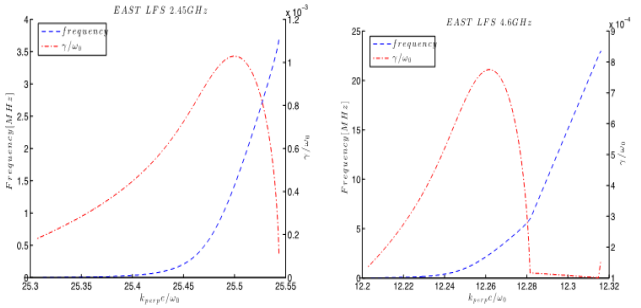

Fig. 11 Calculated frequencies and growth rates (left:2.45 GHz, right: 4.6GHz)(LHPI)

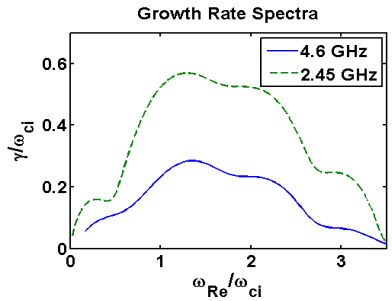

Fig. 12 PI growth rate (n_{ea} = 5×10^{18} m^{-3}, T_{ea} = T_{ia} = 30 eV, B_t = 1.83 T, P_{rf}= 2.91 MW/m^2, $n_{//0}$ = 2, $n_{//quasi-mode}$ = 7*)(MIT code)*

The LH^{star} suite of numerical codes [2, 30] has been further utilised for calculating the driven current profile. In order to model the deposition profiles, and taking into account the above PI code results, the LH power spectrum broadened by the PI mechanism has been considered as initial spectrum, in place of that launched by the antenna. Namely: p_{PI} =20%, $n_{//max}$ =30, for 4.60 GHz, and p_{PI} =50%, $n_{//max}$ =40, for 2.45 GHz have been respectively considered. Preliminary results are shown in Fig. 13. For the case of 4.60 GHz, it is seen that the PI-produced spectral broadening mechanism significantly reduces (of about 60%) the fraction of the power coupled by the antenna that is capable penetrating into the plasma core, but LH current is usefully driven within the radial outer half of plasma. Conversely, owing to the more pronounced PI-produced spectral broadening at 2.45 GHz, a more marked effect of parasitic RF power absorption at the plasma edge is expected to occur. In this case, most

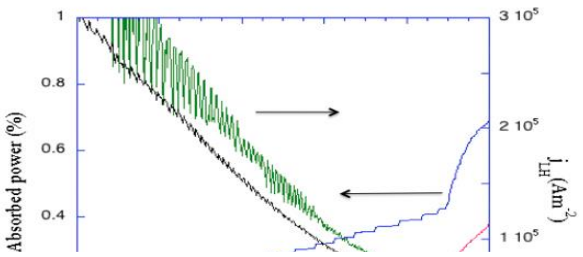

Fig. 13 Radial profiles of the RF power fraction for f=4.60 (blue) and f=2.45 GHz (red), LH-driven current density for f=4.60 GHz (green) and f=2.45 GHz (black) (Coupled RF power:

coupled RF power (about 80%) is deposited in the SOL and cannot contribute to useful LHCD mechanism, leading to a different LH current profile. Such result is consistent with the much weaker LHCD effects that are routinely observed on EAST when operating with the 2.45 GHz frequency, in comparison with the 4.60 GHz case. The results modelled by LH^{star} are also consistent with the much more pronounced phenomena of spectral broadening displayed by data of RF probe measurements available at the two frequencies (see Fig. 3), indicating a stronger PI behavior with 2.45GHz wave.

In JET, a new Ray Tracing (RT)/ Fokker-Planck (FP) package [31], with a real 2D geometry accounting for the plasma boundary and launcher shape and a new 3D relativistic bounce averaged FP code, has been developed for LH power deposition analysis and the main results are shown in Fig. 14. Power deposition profiles from the code are compared to experimentally assessed profiles from modulated LH experiments [32] and ECE analysis data [33]. Calculations are in a reasonable agreement with experimental data at low (#77609) and high (#77612) density. The code cannot reproduce absorption at the cold periphery ($0.6<\rho<0.8$) in both cases whereas in addition to this at high density (#77612) the calculated core absorption ($\rho<0.2$) is much higher than experimental results. Simulations with broadened initial $N_{||}$ spectra (i.e. upshift of $N_{||}$ up to 2.5) resulted in more consistent deposition in the periphery with numerical results matching experimental data up to $\rho\approx0.7$.

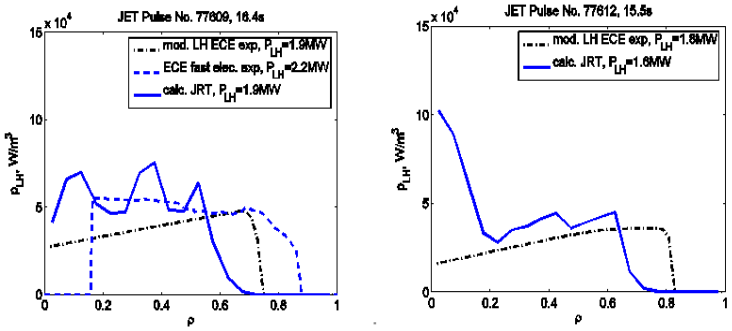

Fig. 14 Data analysis with a real 2D geometry code, 3.4T, low ($2.4x10^{19}m^{-3}$, left) and high ($3x10^{19}m^{-3}$, right) density

4. Conclusions and discussion

Progress in understanding LHCD at high density has been made through multi-machine experiments and modeling, focused on application in ITER. The driven current in the core has been enhanced by reducing neutral density at the plasma edge. The edge temperature is thereby increased and the effects of PI and CA are reduced. The effect of PI is also mitigated by higher LH operating frequency. These effects, plus stronger single-pass damping that will lessen the effects of CA, all points favorably to the application of LHCD in ITER. It is important to point out that, for these joint experiments, C-Mod and FTU are operated at high field and high density ($5\text{-}20\times10^{19}m^{-3}$) whereas EAST and JET are operated at medium field and lower density ($2\text{-}4\times10^{19}m^{-3}$). Although these LHCD experiments span more than an order of magnitude in density and about a factor of five in toroidal magnetic field, they can be usefully characterized in terms of (f_{pe}/f_{ce}) (see Fig. 15), which is the fundamental dimensionless parameter that determines wave accessibility, wave penetration, and wave refraction. Note that for these experiments (f_{pe} / f_{ce}) covers a range from 0.35 to ≥ 1.0 which easily brackets the value of 0.5-0.6 expected in the ITER steady state Scenario 4, thus giving some confidence in the extrapolation of results found in these experiments to ITER.

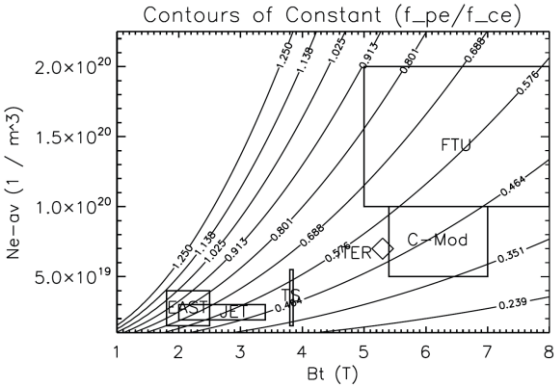

Fig. 15 f_{pe}/f_{ce} contours for different devices

These joint experiments have shown the importance of SOL parameters in determining parasitic losses from PI, CA, and SDF, especially in regimes where damping of the LH wave is weak. However experiment and simulation support the expectation that the significantly hotter electron temperatures in ITER should help to mitigate these mechanisms.

Acknowledgements: This work is supported by the National Magnetic Confinement Fusion Science Program of China (Grant No. 2015GB102003, 2013GB106001B, 2013GB112003), the National Natural Science Foundation of China under Grant No. 11175206, 11305211 and 11275233, Hefei Science Center CAS (2015HSC-UE005, 2016HSC-IU008), and the JSPS-NRF-NSFC A3 Foresight Program in the field of Plasma Physics (NSFC No. 11261140328). Part of the work was conducted on the Alcator C-Mod tokamak, a DoE Office of Science user facility, and is supported by USDoE awards DE-FC02-99ER54512, DE-AC02-09CH11466, and DoE Grant DE-SC0010492. It is partly supported by the China-Italy and the China-France Collaboration program. We also give thanks to the support from the IOS TG of the ITPA. This work has been carried out within the framework of the EUROfusion Consortium and has received funding from the Euratom research and training programme 2014-2018 under grant agreement No 633053. The views and opinions expressed herein do not necessarily reflect those of the European Commission.

References:

[1] Litaudon X *et al*, 2002, *Plasma Phys. Contr. Fusion* **44** 1057.
[2] Cesario R et al., 2010, *Nature Communications*, 1 (5) 55.
[3] Cesario R, et al., 2004, *Phys. Rev. Lett.* **92** 175002.
[4] Bonoli P.T., and Englade, R.C. 1986 *Phys. Fluids* **29** 2937.
[5] Peysson Y., et al 2011 *Plasma Phys. Contr. Fusion* **53** 124028
[6] Bonoli, P.T., and OTT, E. 1982*Phys. Fluids***25** 359.
[7] Fisch N J and Boozer A H 1980 *Phys. Rev. Lett.* **45** 720.
[8]Liu F K, et al., 2015 *Nucl. Fusion* **55** 123022.
[9] Ding B J et al., to be submitted to *Phys. Rev. Lett.*
[10] Lyu B. et al., 2014 *Rev. Sci. Instrum.* **85** 11E406.
[11] Faust I. et al., 2016 *Phys. Plasmas* **23** 056115.
[12] Klepper C. C.et al., 2013 *Phys. Rev. Lett.* **110** 215005.
[13] Baek S. G. et al., 2016 *Phys. Plasmas* **23** 050701.
[14] Baek S.G. et al., 2015 *Nucl. Fusion* **55** 043009.
[15] Castaldo C, et al., 2016 *Nucl. Fusion* **56** 016003.
[16] Goniche M et al., *Edge plasma–lower hybrid wave interaction and current drive efficiency*, 42nd EPS conference, Lisbon, Portugal, 22-26 June, 2015
[17] Cesario R et al., 2011, *Plasma Phys. Contr. Fusion* **53** 085011.
[18] Barbato E, et al., 2014 Nuclear Fusion **54** 123009
[19]Ding B J et al., 2013 *Nucl. Fusion* **53** 113027.
[20]Cesario R, et al., 2014 *Nucl. Fusion* **54** 043002.
[21]Takase Y. and Porkolab M., 1983, *Phys. Fluids* **26** 2992.
[22] Baek S. G., et al., 2014, *Phys. Plasmas* **21**, 061511.
[23] Porkolab M. 1977 *Phys. Fluids* **20** 2058.
[24] Liu C.S. et al 1984 *Phys. Fluids* **27** 1709.
[25] Mumgarrd B. et al., 2015 *Bull. Am. Phys.* **60** CP12.019.
[26] Decker J., et al., 2014 *Phys. Plasmas* **21**, 092504.

[27] Peysson Y et al., 2016 *Plasma Phys Contr. Fusion*. **58** 044008.
[28] Wallace G.M., et. al., 2012 *Phys. Plasmas* **19** 062505.
[29] Shiraiwa S., et al., 2015, AIP Conf. Proc. **1689** 030016.
[30] Cesario R et al., 2014,*Nucl. Fusion* **54** 043002.
[31] Kirov K et al 2016 *Plasma Phys Contr. Fusion* **58** 101205.
[32] Kirov K et al 2010 *Nucl. Fusion* **50** 075003.
[33] Kirov K et al 2012 *Plasma Phys Contr. Fusion* **54** 074003.